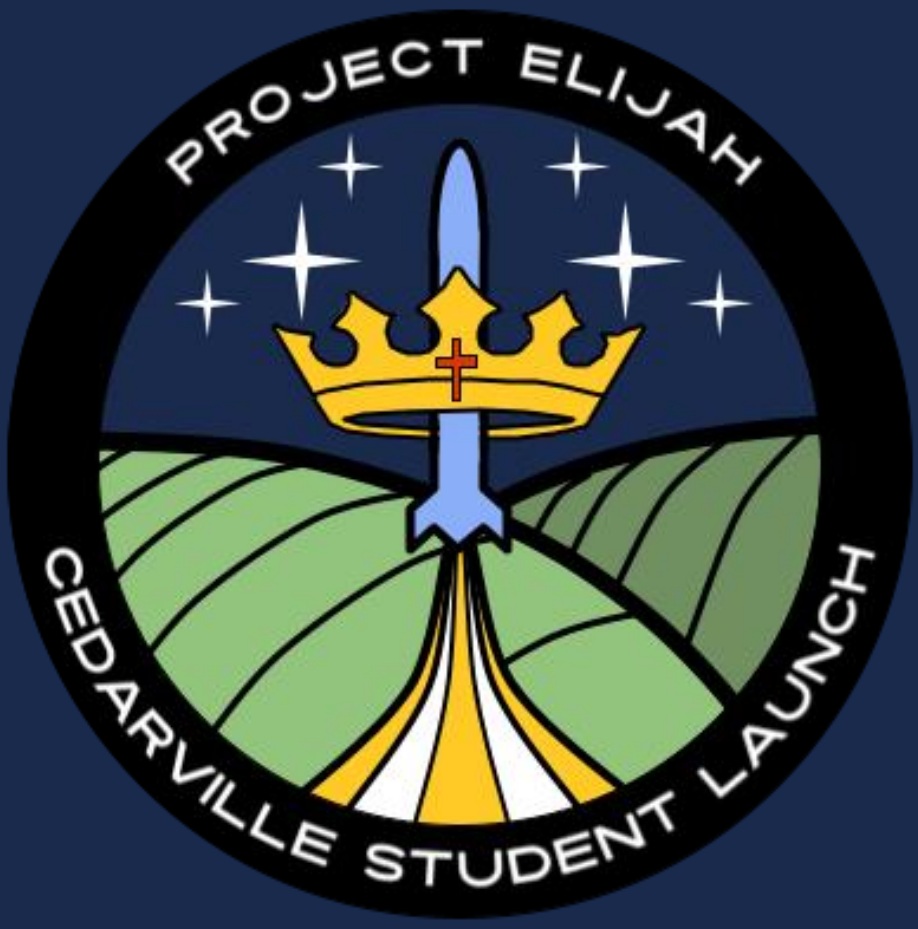

Project Elijah

Flight Readiness Review Addendum

Cedarville Student Launch 2024-2025

Cedarville University
251 N. Main St.
Cedarville, OH 45314
April 14, 2025

Table of Contents

1. Summary of FRR Addendum 5
1.1. Team Summary 5
1.2. Launch Vehicle Summary 5
1.3. Purpose of Flight(s) 6
1.4. Flight Summary Information 6
1.5. Changes Made Since FRR [DANIEL & ECES] 8
1.5.1. Changes Made to Vehicle Design 8
1.5.2. Changes Made to Payload Design 10
2. Payload Demonstration Flight Results 10
2.1. Primary Payload Mission Success Criteria & Sequence [ECEs] 10
2.2. Primary Payload Retention System [ECEs] 11
2.3. Primary Payload Flight Results [ECEs] 12
2.4. Secondary Payload Mission Success Criteria & Sequence 13
2.5. Secondary Payload Retention System 14
2.6. Secondary Payload Flight Results 14
2.7. Future Flight Considerations 16
3. Vehicle Demonstration Re-Flight Results 17
3.1. Mission Success Criteria & Flight Sequence 17
3.2. Demonstration Flight Overview 18
3.3. Flight Data 20
3.4. Vehicle Recovery Discussion 21
3.5. Flight Analysis 26
3.6. Future Flight Considerations 26

FRR Acronym References

Acronym	Full Name
AB	Airbrakes Subsystem
AGL	Above Ground Level
ANSI	American National Standards Institute
APRS	Automatic Packet Reporting System
CAD	Computer Aided Design
CDR	Critical Design Review
CE	Chief Engineer
CFD	Computational Fluid Dynamics
CG	Center of Gravity
CNC	Computer Numerical Control
COTS	Commercial-Off-the-Shelf
CP	Center of Pressure
CSL	Cedarville Student Launch
CSO	Chief Safety Officer
DMM	Digital Multimeter
EPL	Engineering Project Laboratory
FAA	Federal Aviation Administration
FBD	Free-Body Diagram
FCC	Federal Communications Commission
FDM	Fused Deposition Modeling
FEA	Finite Element Analysis
FEM	Finite Element Method
FMEA	Failure Modes and Effect Analysis
FRR	Flight Readiness Review
GLOW	Gross Lift-Off Weight
GPS	Global Positioning System
HPR	High Power Rocketry
HPRSC	High Power Rocketry Safety Code
I^2C	Inter-Integrated Circuit
IDE	Integrated Development Environment
LED	Light Emitting Diode
LiPo	Lithium-Ion Polymer
LO	Launch Officer
MGA	Mass Growth Allowance
NAR	National Association of Rocketry

NASA	National Aeronautics and Space Administration
Ni-Cd	Nickel–Cadmium
OD	Outer Diameter
PCB	Printed Circuit Board
PDR	Preliminary Design Review
PETG	Polyethylene Terephthalate Glycol
PLA	Polylactic Acid
PM	Project Manager
PPE	Personal Protective Equipment
PTT	Push-to-Talk
RRC	Rocket Recovery Controller
RSO	Range Safety Officer
RTC	Real-Time Clock
SDS	Safety Data Sheet
SDK	Software Development Kit
SL	Student Launch
SPI	Serial Peripheral Interface
STEM	Science, Technology, Engineering, and Mathematics
TRA	Tripoli Rocketry Association
USLI	University Student Launch Initiative
VDF	Vehicle Demonstration Flight
WBS	Work Breakdown Structure
WSR	Wright Stuff Rocketeers

List of Figures

Figure 1.4.1. (Left) CSL's NAR mentor installing the ignitor for Chariot flight #3; **(Right)** Chariot shortly after rail exit on flight #3. 8
Figure 2.2.1. Front and back view of payload inside airframe and nosecone. 11
Figure 2.5.1. Airbrakes retention system. 14
Figure 2.6.1. Airbrake actuation during PDF-VDF flight 15
Figure 3.3.1. Altimeter flight profile graph of Chariot flight #3 from primary RRC3 altimeter. 20
Figure 3.3.2. Altimeter flight profile graph of Chariot flight #3 from secondary Easy mini altimeter. 21
Figure 3.4.1. Aerial view of launch and landing sites for Chariot flight #3. Chariot landed 1,317 ft from the launch rail. 22
Figure 3.4.2. (Left) Picture of Eggtimer gps reciever while Chariot is on the launch rail. (**Right)** Eggtimer gps receiver after landing. 22
Figure 3.4.3. As landed configuration of Chariot after flight #3 (drone view on right). 23
Figure 3.4.4. Chariot aft section as landed configuration. 24
Figure 3.4.5. Chariot avionics section as landed configuration. 24
Figure 3.4.6. Chariot forward section as landed configuration. 25
Figure 3.4.7. Chariot forward section and main parachute as landed configuration. 25

List of Tables

Table 1.4.1. Chariot Flight #2 Vehicle Demonstration Re-Flight and Payload Demonstration Flight overview table. 6
Table 1.4.2. Chariot flight #3 predicted vs actual recovery metrics 7
Table 1.5.1. Recovery system changes summary. Note the change in parachute and black powder charges. 9
Table 1.5.2. Airbrakes DC motor changes summary. 10
Table 3.4.1. Calculated kinetic energy of each independent section upon landing. 26

1. Summary of FRR Addendum

1.1. Team Summary

Team Info	Cedarville Student Launch Team (CSL) 251 North Main Street, Cedarville, OH 45314	**Final Launch Plan**	5995 Federal Road, Cedarville, OH 45314 WSR, NAR #703 Dave Combs, President April 26, 2025
Mentor Info	Dave Combs – #86830 – High HPR Level 2 Email: davecombs@earthlink.net Phone Number: (937) 248 – 9726	**Backup Launch Plan**	5995 Federal Road, Cedarville, OH 45314 WSR, NAR #703 Dave Combs, President April 27, 2025
NAR Section	NAR #703 Wright Stuff Rocketeers (WSR)	**FRR Addendum Hours**	**85**

1.2. Launch Vehicle Summary

Target Apogee	**4100 ft**
Competition Launch Motor	**Aerotech K1000T-P**
Fore Section Length / Weight	**30 in / 6.65 lb**
Avionics Bay Section Length / Weight	**27.25 in / 3.98 lb**
Aft Section Length / Weight	**56.95 in / 12.43 lb**
Dry Mass with / without Ballast	**22.37 lb / 21.61**
Wet / Burnout / Landing Masses	**28.05 lb / 25.72 lb / 25.72 lb**
Recovery System	**15” Elliptical Drogue / 8 ft Toroidal Main**
Rail Size	**1515 / 12ft Long**

1.3. Purpose of Flight(s)

The flight submitted with this FRR Addendum was conducted to fulfill the requirements of a Vehicle Demonstration Re-Flight and Payload Demonstration Flight. This singular flight will be summarized in sections 2 and 3 of this report, separated into portions detailing payload and launch vehicle performance. The system was flown on April 8th, a few hours following CSL's FRR presentation, in full competition configuration with an Aerotech K1000T-PS motor, the same motor that will be used for the competition flight.

1.4. Flight Summary Information

The third flight of Chariot was conducted on April 8, 2025, and was intended to fulfill the requirements of the Vehicle Demonstration Re-Flight and the Payload Demonstration Flight. Liftoff took place at 8:13 PM for a sunset launch. The rocket was observed to have experienced some wobble and corkscrewing during the motor burn. This was probably due to one of the airbrake flaps not being completely flush with the airframe of the rocket causing some instability during liftoff. A nominal coast phase and recovery sequence was observed with Chariot landing at a speed of 15.5 ft/s, 1317 ft from the launch site 79.6 seconds after launch. The onboard RunCam did not record video of the launch, it stopped recording 47 seconds after being turned on while the rocket was on the launch rail. The reason for the RunCam malfunctioning has not been determined and it has worked as expected in testing both before and after the launch. Tables 1.4.1 and 1.4.2 contain a summary of the relevant information for this flight and Figure 1.4.1 contains Chariot on the launch rail before launch as well as Chariot just after rail exit.

Table 1.4.1. *Chariot Flight #2 Vehicle Demonstration Re-Flight and Payload Demonstration Flight overview table.*

Date of flight	April 8, 2025. 8:13 PM EST
Location of flight	WSR club launch site: 5995 Federal Rd, Cedarville, OH 45314
Launch conditions	Temperature: 37° F Wind: 6 mph (gusts 12 mph Visibility: >10 miles Cloud cover: Clear Relative humidity: 45%
Motor	Aerotech K1000T-P
Ballast flown	0.765 lb (347 g)
Payload status	Active

Air brake status	Active
Official target apogee	4100 ft
Predicted apogee	4100 ft
Measured apogee	3890 ft
Descent time	64.8 s
Drift distance	1317 ft
Drogue deployment	Apogee & apogee +1 s
Main deployment	600 ft & 550 ft

Table 1.4.2. *Chariot flight #3 predicted vs actual recovery metrics*

Section	Wet Mass (lbs)	Landing Mass (lb)	Predicted Drogue Descent Rate (ft/s)	Predicted Main Descent Rate (ft/s)	Predicted Landing Kinetic Energy (ft*lbf)	Actual Drogue Descent Rate (ft/s)	Actual Drogue Kinetic Energy (ft*lb)	Actual Main Descent Rate (ft/s)	Actual Landing Kinetic Energy (ft*lbf)
Forward	6.65	6.65	175	14.3	21.1	86.1	766.7	15.5	24.8
Avionics	3.98	3.98	175	14.3	12.6	86.1	458.3	15.5	14.9
Aft	14.76	12.43	175	14.3	39.5	86.1	1432.6	15.5	46.4

Figure 1.4.1. (Left) *CSL's NAR mentor installing the ignitor for Chariot flight #3;* ***(Right)*** *Chariot shortly after rail exit on flight #3.*

1.5. Changes Made Since FRR

1.5.1. Changes Made to Vehicle Design

The ballast, epoxied in place in the nosecone, has been reduced to 300g after final maturation of the full-scale launch vehicle design. Additionally, the heat-set inserts used to fasten the nosecone to the airframe were replaced with threaded nuts epoxied into the interior of the printed nosecone. This replacement was brought on by weaknesses introduced to the nosecone by melting the PETG surrounding the inserts.

CSL also updated the recovery system to account for excessive landing velocities and kinetic energies experienced during the first VDF attempt. Due to the finalized weight of the system, the main parachute size and profile have been changed to achieve a sufficient coefficient of drag. This

change in main parachute required updated black powder charge sizes, which have been adjusted. After consideration of counseling received from NASA during the FRR presentation, CSL has updated all backup black powder charges to have a fixed increase of 25% instead of a ½ gram increase as in previous flights. These changes in the recovery system have been summarized in Table 1.5.1 below.

Table 1.5.1. *Recovery system changes summary.*
Note the change in parachute and black powder charges.

Chute Specifications	New Chute	Old Chute
Size & Type	8ft Toroidal	7ft Parabolic
Weight Rating	29.8 lbs	25 lbs
Coefficient of Drag	2.2	0.9
Recovery Element	**Original Black Powder Mass**	**New Black Powder Mass**
Main Primary	5.0	3.5 g
Main Redundant	5.5	4.5 g
Drogue Primary	3.3	3.3 g
Drogue Redundant	3.8	4.0 g

CSL had difficulty identifying an issue with the airbrake's electronics-can fitting in the rocket stack. On the day of the flight on 4/8/25, the team found that this was due to the airbrakes PCB components being subtly different from those of the CAD model used in the full Chariot assembly, resulting in some hardware putting pressure on the PCB itself and preventing the rocket from being assembled easily. Flipping the shock cord mount plate gave an extra ~0.25" of clearance inside the electronics can and allowed the rocket to be fully assembled.

The airbrakes have had some small design changes, discussed in the FRR presentation. The airbrakes flaps have been reduced in length by $1/8^{th}$ of an inch to ensure their actuation does not interfere with the airframe, the PETG 3D printed anchor slider has been replaced with a reinforced DMLS aluminum 3D print, and the previous motor has been replaced with a lower rpm, higher torque motor.

Table 1.5.2. *Airbrakes DC motor changes summary.*

AB Motor Specifications	New Motor	Old Motor
Voltage	24 V	12 V
RPM	200	300
Produced Force Per Flap	5.0 lb	4.4 lb
Time	2.1 s	N/A*

*This motor failed a test because it could not lift 4.4 pounds per flap, hence its replacement.

1.5.2. Changes Made to Payload Design

No significant changes were made to the payload design since the FRR. The team primarily finalized software functionality and bug fixes, rather than changing designs completely.

2. Payload Demonstration Flight Results

2.1. Primary Payload Mission Success Criteria & Sequence

The mission of the primary payload, as stated in the Student Launch Handbook Section 4.1, is to safely hold four STEMnauts and to transmit flight and landing information to a receiver over radio after landing. In order to do so successfully, the payload must first collect flight data for the entire launch duration. Then that data must be processed, formatted, and encoded for transmission via radio on the 2-meter band. The payload must also remain structurally intact to protect the four onboard STEMnauts.

The following success criteria provide testable and verifiable benchmarks for the overall mission. A fully successful payload flight will be one in which all of the following criteria as well as all of NASA's specific payload verifications are fulfilled.

P.1 Payload survives vehicle landing to be able to perform post-flight operations.
P.2 Payload has sufficient battery power for pre-flight, in-flight, and post-flight operations.
P.3 Payload sensors all deliver accurate data to the microcontroller.
P.4 Payload transmits APRS packets from the rocket's landing site to the launch site receiver.
P.5 Payload transmits decodable telemetry data using the standard APRS protocol.

The primary payload goes through five phases during the course of the mission, each one of which is triggered by changes in altitude or acceleration as sensed by the payload's onboard sensors. The Raspberry Pi Pico microcontroller performs different operations during each phase of the flight. These flight phases are shared with the secondary payload systems.

The first phase is Preflight, which is entered when the system is turned on. During this phase, the calibration data must be set, and the microcontroller constantly checks that the microSD card and

all sensors are interfacing correctly and no faults are detected. When this is true, the Pico activates the speaker and LEDs to indicate that it is ready for launch.

The second and third phases are Burn and Coast. The Burn phase is entered when the Pico detects an altitude of at least thirty meters above the ground, and an acceleration magnitude of fifty meters per second squared or greater within the last five seconds. Coast phase is entered once the altitude exceeds 350 meters above the ground, or 1.4 seconds after entering Coast, whichever is sooner. During these phases, the primary objective of the payload is simply to collect and store flight data.

The fourth phase is Descent, which is triggered when a continuous decrease in altitude is detected. When this occurs, the Pico records the maximum apogee that was reached and continues to log flight data.

The payload's final phase is Postflight, which occurs when the payload detects that it has remained still for a period of time. During the Postflight phase, the Raspberry Pi Pico on the main PCB records the time of landing and uses an APRS library to encode the data to be transmitted; the transmitter's PTT is then activated and the APRS packets are all transmitted out every thirty seconds. The Pico on the override PCB enables the transmitter's PTT for five minutes after landing to allow the main PCB to send transmissions.

2.2. Primary Payload Retention System

The retention system for the primary payload can be seen in Figure 2.2.1. The lower section of the payload is enclosed by translucent covers, while the upper section is encircled by the nosecone. The payload's largest diameter only allows it to slide into the airframe as far as the airframe overlaps, and the nosecone retains it from above. Two fasteners are used to completely secure it from the outside of the airframe, and the bulkhead below seals off the payload compartment.

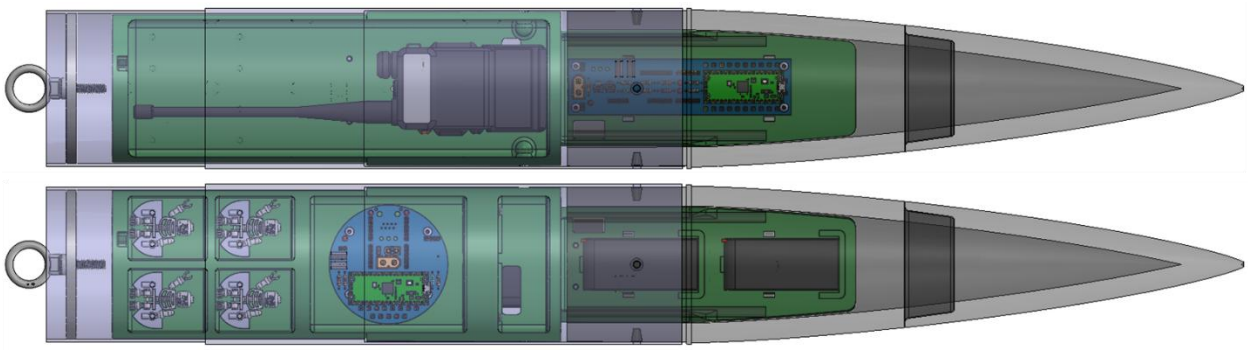

Figure 2.2.1. *Front and back view of payload inside airframe and nosecone.*

2.3. Primary Payload Flight Results

All of the payload's mechanical systems functioned correctly. The payload assembly included the translucent shields which provided covering for all internal components while still allowing for the LED indicators to be visible. All payload hardware survived the flight with no visible damage. The STEMnauts remained perfectly in their capsule and the payload was able to be easily extracted from the nosecone and airframe.

Nearly all of the payload's software system operated correctly. The section of the program that deals with flight phase transitions was tested ahead of time with simulated flight data, and it passed the test perfectly. The payload was then calibrated correctly and the software indicated that all systems were ready for launch. When the rocket launched, the main PCB detected an increase in acceleration and altitude and proceeded through the flight phases as expected.

The override PCB did not change through the flight phases as intended. Though the flight phase controller is shared between all three computer systems, data is retrieved from different controllers. In the code, this is implemented as a pure virtual class with implementations for data collection. One piece of data that the controller checks for is if the system is calibrated. This is to prevent changing flight phases with the random data that comes from an uncalibrated system. The override PCB stores if it has been calibrated as an unsigned 1-byte integer reading 255 for calibration, or zero when it is uncalibrated, however, the check within the flight phase controller implementation read back an 8-byte floating point, which is undefined behavior. The random bits in memory likely caused the floating point to always read as less than zero, so the override never considered itself calibrated. This check is skipped while using test data, since it was thought that the calibration values would be meaningless with fake data. The override PCB's code has changed to check calibration, even with test data.

Both circuits successfully logged and stored all data which allows the payload team to interpret and recreate the flight for further software testing and validation. When the rocket landed, the main PCB encoded the collected data into APRS packets and sent them to the transmitter. A record of this is also stored in the log.

The payload's electrical system worked as intended. The two LiPo batteries stayed above 70% charged for the entire mission and the transmitter's battery remained fully charged. All electrical connections remained intact for the flight and the sensors provided accurate data to the microcontrollers. The payload's radio transmitter setup is designed electrically to "fail safely", meaning that no one failure will ever cause the transmitter to activate when it is not permitted to. This means that when the main PCB attempts to activate the transmitter's PTT while the override PCB believes that the rocket is still on the launchpad, the override PCB does not permit it, and vice versa. This is the sequence of events which occurred during the flight, where the main PCB correctly sent the APRS packets to be transmitted but the override PCB prevented them from being sent.

Due to the success of the primary PCB and secondary payload (which share the same code), and the fact that the altitude data collected by the override PCB matches the data collected by the primary PCB and secondary payload, the team is confident that the override PCB will successfully detect each phase of flight and allow transmission of data for five minutes upon landing, as intended. The team intends to do an integrated test, by using the same test data for both the main and override PCB's, at the same time, to ensure that both detect landing at similar times, and data transmission is permitted for the intended time.

2.4. Secondary Payload Mission Success Criteria & Sequence

AB.S.1 Airbrake deployment during flight is confirmed.
AB.S.2 Airbrakes are stowed within ±2 seconds of apogee.
AB.S.3 Rocket apogee lands within ±25 feet of target altitude.
AB.S.4 Confirmation of drag flaps actuation via the onboard camera.
AB.S.5 Drag flaps are located no further than 2 inches behind the Center of Pressure (CP).
AB.S.6 No components experience mechanical failure during any stage of flight.
AB.S.7 No electrical brownouts or blackouts occur.
AB.S.8 Flight data is recorded and retrieved.

The rocket altitude needs dynamically altered during flight. The secondary payload, the system's airbrakes, control velocity in flight by inserting a control surface into an airstream to increase coefficient of drag. The secondary payload detects phases of flight using the same code as both primary payload PCBs. In a constant feedback loop during the coast phase the sensors read the pressure (altitude) to determine the velocity of the rocket and match the coefficient of drag (Cd) of the rocket to the Cd for a predetermined path by inserting the flaps into the airstream. This predetermined path was calculated using a P controller.

Due to the actuation of the rotary encoder, as seen in Figure 2.6.1, and because the rocket reached an apogee much lower than predicted without airbrakes, the AB.S.1 objective has been met. As seen in Figure 2.6.1 the flaps are stowed as fast as possible once the rocket hit apogee, less than 2 seconds long. Thus, success criteria AB.S.2 was satisfactorily met. The final apogee, as recorded by the primary scoring altimeter, was $3890[ft]$. Thus, the airbrakes did not successfully fulfill the success criterium AB.S.3. Because the onboard camera turned off before flight, success criterium AB.S.4 could not be measured. The Center of pressure (CP) was located at 72.05 [in] away from the nosecone with no deployment and during full flap deployment the CP was located 71.39 [in] from the nosecone. Because the airbrakes were located 71.69 [in] from the nosecone, the rocket was stable no matter how far the airbrakes deployed and passed AB.S.5. Success criteria AB.S.6 was passed because no components broke during flight. During the flight data was taken with no discontinuity in time. This indicates that power was not lost during the flight. Thus, success criteria AB.S.7 was passed. Lastly, the flight data was collected and now it is in the report, see Figure 2.6.1, thus success criteria AB.S.8 was passed.

2.5. Secondary Payload Retention System

Like the motor retention system, the airbrake secondary payload was retained in the rocket by seven 10-32 screws that were passed by the airframe and threaded into heat set inserts that set inside the airbrakes mounting points. These screws held the motor mount on the bottom of the payload and the encoder mount on the top side of the mechanical system of the payload. The flaps were fastened into place using two or three 4-40 screws per flap. These screws can be seen in figure 2.5.1. The motor mount only held three 10-32 screws because the electrical motor controller caused the absence of one screw hole. Because of manufacturing defects in two of the ternary links, there were only two screws in the respective flaps.

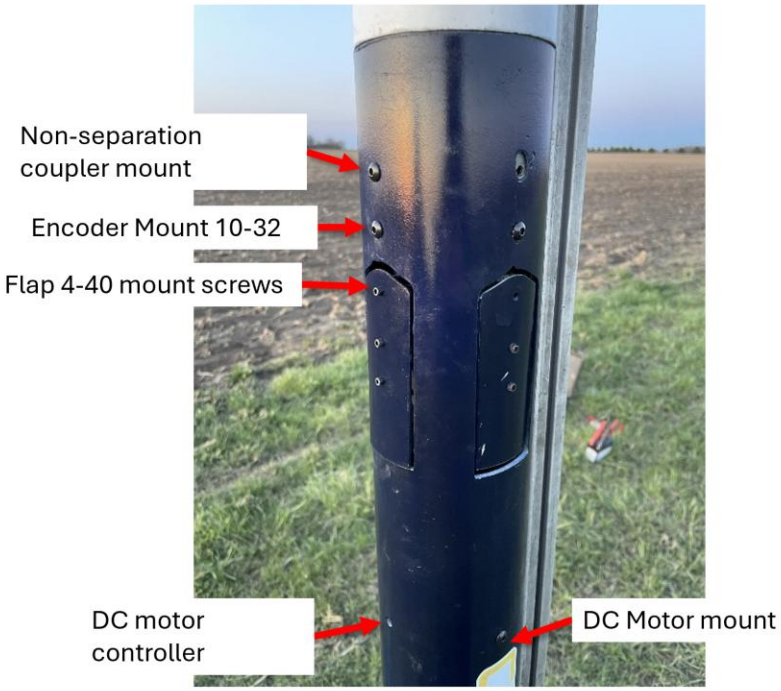

Figure 2.5.1. *Airbrakes retention system.*

Between the airbrakes and the airframe was a coupler cut to size to reinforce the structure of the airframe. This coupler was not removed but instead was used only to thicken the airframe and provide structural reinforcement in the unlikely event of a landing with higher energy than anticipated. Above the airbrakes is a non-separation coupler. This held the electronics canister for the airbrakes and allowed them to be inserted and removed from the airframe with minimum difficulty.

2.6. Secondary Payload Flight Results

Figure 2.6.1 shows the data recorded from the VDF/PDF. The altitude looks as expected through its trajectory. Unfortunately, it went too low at a final apogee of 3890 [ft]. This is because of the unexpected behavior of the airbrakes due to data filtering. Various algorithms were used to control the airbrakes during coast phase. The altitude (pressure) was used in the P controller to minimize

the error between the current velocity and the desired velocity at the current altitude. One BMP280 sensor was used to collect this data, and it was accurate within eleven feet over the primary altimeter and eight feet under the payload.

Pressure readings were taken about every 40 milliseconds to provide accurate altitude measurements over time. (Note: the time step is not constant, the median was 41.24 and the mean is 42.5.) The velocity was then calculated using the change in pressure over time, which would be dx/dt (a derivative). However, the pressure did not always change between successive measurements, resulting in a calculated velocity of zero for several iterations. This caused the controller to command a zero flap-angle. When the pressure eventually changed, the simple velocity calculation—based on the difference in pressure over the fixed time step—produced an unrealistically high velocity. In response, the controller commanded the flaps to the maximum angle. This cycle repeated until the velocity decreased enough for the rocket to fall within the acceptable range for the controller to resume following its predetermined trajectory. At this point, though, the rocket was going too slow to meet its altitude requirement.

It can be reasoned, because the data acquired, that the airbrakes electromechanically worked as intended. The safety of the rocket is contingent on a foreseeable case. If the airbrakes are not stowed within 2 seconds of apogee then the shock chords can be tangled in the airbrakes and this would pose a recovery problem. Because the electromechanical systems had no problems then there is no safety to the rocket or the bystanders.

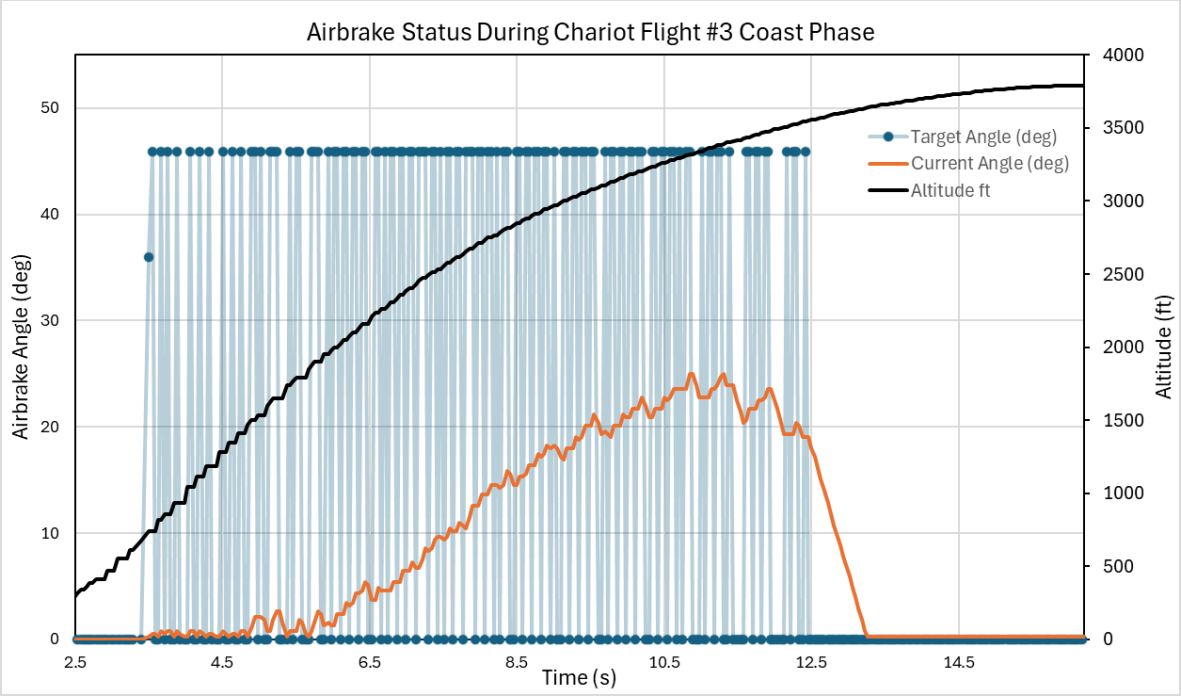

Figure 2.6.1. *Airbrake actuation during PDF-VDF flight.*

2.7. Future Flight Considerations

After launch the data was analyzed to determine a more accurate process for calculating velocity. Instead of taking the last iteration and current iteration to calculate velocity, the function will keep time and wait to detect a pressure change. When there is a pressure change, then it will take the difference between the last pressure read and the current pressure and divide this by the total amount of time between pressure readings.

Because taking a finite derivative of position results in error, integration of acceleration data was determined to be a conceivable method for calculating velocity alongside the previous method for increased accuracy. Thus, two methods will be used on board to calculate velocity. A test has been conducted with the data from this launch to determine the accuracy of the acceleration integration to get the velocity. It was determined to be reasonably accurate when compared to known data. Another concern with using the acceleration to calculate the velocity is that error accumulates overtime. If there is a bias to the accelerometer or the data or something the error accumulates only ever gets worse. The velocity will be calculated using two different methods and these two methods will be averaged during flight to determine the best guess of rocket state space.

The wrong equation was used to calculate the pressure during the flight, this created an error of approximately 100 [ft] at apogee. This is due to pressure and temperature conditions on the ground. With the correct equation implemented in post processing, the pressure gives an error with less than 10 [ft].

No hardware on the airbrakes were damaged during flight and the electromechanical system worked as intended. The control system was not functionally tested because the state space model did not work as intended. The state space model being the process to determine the state of pressure, velocity, acceleration, and temperature of the rocket at any point in time. The only factor the faulty state space model effects is correct apogee prediction. During launch, the flight phase controller detected all phases successfully.

No hardware on both the primary and secondary payloads was damaged during the flight, meaning both systems are ready to launch again using the same hardware components.

The CSL team learned that it is incredibly valuable to have the speakers onboard the PCBs, allowing us to confirm before launching that all systems are turned on and functioning without faults. The payload team also learned that the effect of these speakers on other sensors should be checked carefully to minimize errors brought about by the speaker’s large instantaneous current draw.

3. Vehicle Demonstration Re-Flight Results

3.1. Mission Success Criteria & Flight Sequence

Mission success of the Vehicle Demonstration Re-Flight will involve fulfilling all remaining CSL and NASA requirements such that the launch vehicle is proven to be completely capable of fulfilling its mission. This mission is for the launch vehicle, Chariot, to safely fly the STEMnaut flight capsule, Elijah, to its desired apogee, and after landing, transmit capsule and landing site data to a designated receiver. For the vehicle to be completely successful, it must survive such that it can be immediately re-launched after appropriate energetics have been replaced.

Previous flights have confirmed the overall capability of the launch vehicle's function, with this flight setting out to absolutely confirm the system's ability to land with appropriate impact kinetic energies, a successfully transmitting GPS unit, and a successfully functioning airbrakes system.

A fully successful vehicle demonstration flight will be one in which all the following criteria, as well as criteria stated in requirement 2.19 of the NASA handbook, are fulfilled:

V.1 The full-scale launch vehicle will be able to be sufficiently powered by K class motors.
V.2 CSL will create an iterable and customizable vehicle with an overall modular design.
V.3 CSL will use an onboard camera to get flight footage, having minimal effect on the flight.
V.4 The nosecone will reduce drag acting on the launch vehicle during flight.
V.5 The nosecone will improve flight stability.
V.6 The nosecone will provide strength to the fore section and protection to the primary payload.
V.7 The nosecone will survive landing, remain attached, and be immediately reusable.
V.8 The tailcone will improve launch vehicle performance.
V.9 The tailcone will remain attached and retain the motor tube during all stages of flight.
V.10 The tailcone will survive landing within expected energy and be reusable for re-flights.
V.11 The tailcone will survive heat from flight with minor/no damage and be reusable re-flights.

The launch vehicle has several phases throughout its mission sequence. First is ignition, where the launch vehicle is ignited from a remote launch controller. Then, the launch vehicle flies until the motor stops burning, where it reaches a coasting phase. While coasting, the airbrakes controller activates, and the vehicle enters its apogee control phrase. When the launch vehicle reaches apogee, the recovery phase begins. The drogue chute deployment charge immediately fires (with a backup charge firing one second later). When the vehicle descends to 600ft, the main chute deployment charge fires (with a backup charge firing 50ft lower). When the launch vehicle lands, the primary payload transmission phase begins, further discussed in Section 2.

3.2. Demonstration Flight Overview

Chariot experienced a wobbly ascent in its most recent flight. The team has observed this flight behavior before, and it was attributed to the large amount of ballast (>1 kg) secured in the nosecone at the time. However, since the ballast amount was reduced to 300g, the crooked flight path just clear of the launch rail has been attributed to the airbrake flaps protruding oddly from the airframe. The rocket performed a perfect recovery sequence, firing all charges and fully deploying both recovery devices. Except for some construction defects and an unknown camera error, the only portions of Chariot that did not function as intended were software components involved in the operation of both the primary and secondary payloads: all other payload hardware and vehicle components functioned as intended. Figure 3.2.1 summarizes the conditions of each major subsystem upon rocket recovery.

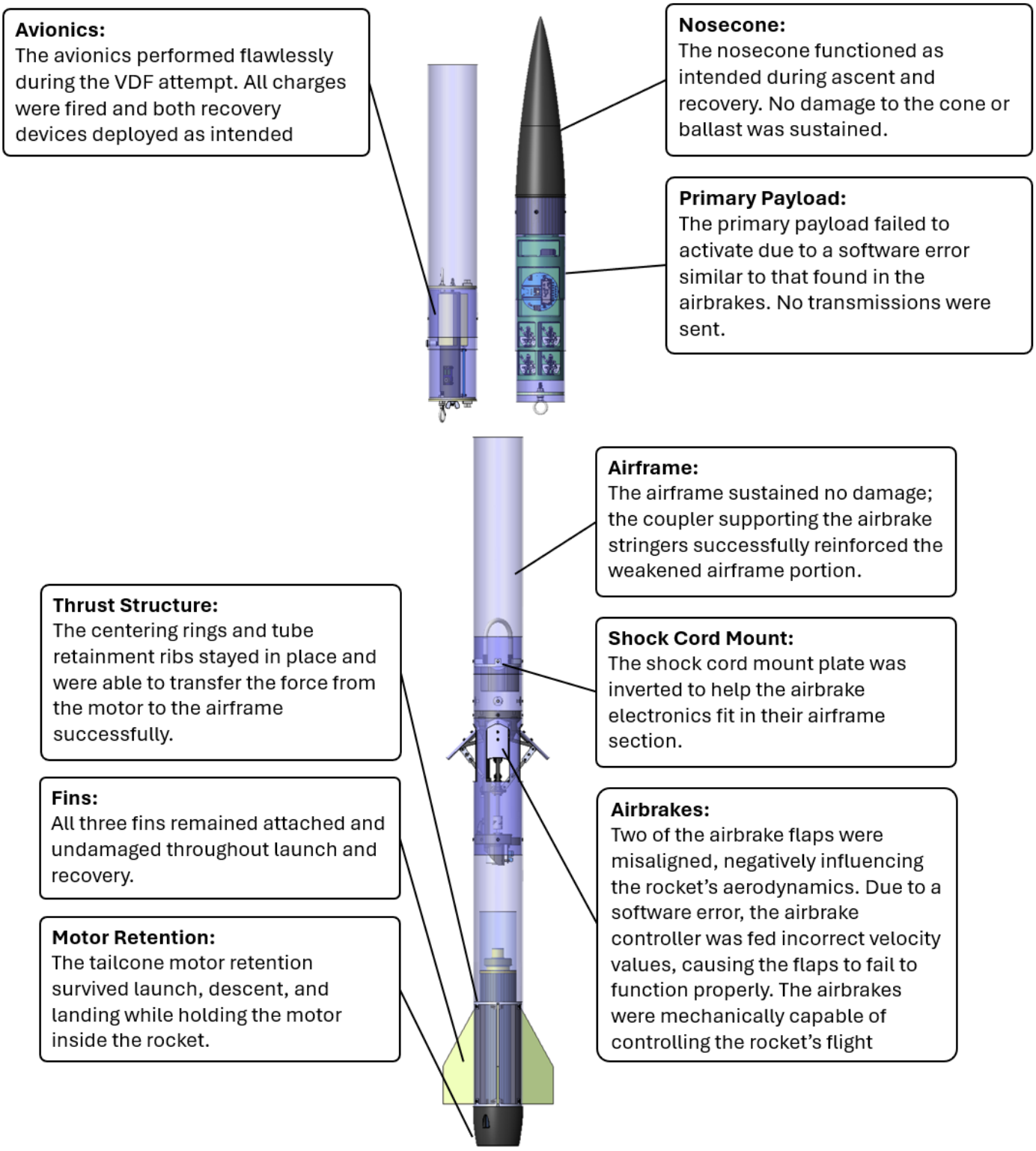

Figure 3.2.1. *Summary of Chariot's subsystem performance during the VDF/PDF attempt.*

3.3. Flight Data

The altimeter flight profile graphs from both the primary RRC3 altimeter and secondary Easy Mini altimeter are shown in Figures 3.3.1 and 3.3.2 respectively. Chariot reached an apogee of 3890 ft as measured by the RRC3 and 3917 ft as measured by the Easy Mini. The landing velocity was found by finding the slope of the altitude vs time during the main parachute descent from the RRC3 altimeter. This landing velocity was calculated to be 15.5 ft/s which is slightly higher than the predicted landing velocity of 14.5 ft/s. All four ejection charges were successfully ignited by the two altimeters and facilitated a nominal recovery sequence.

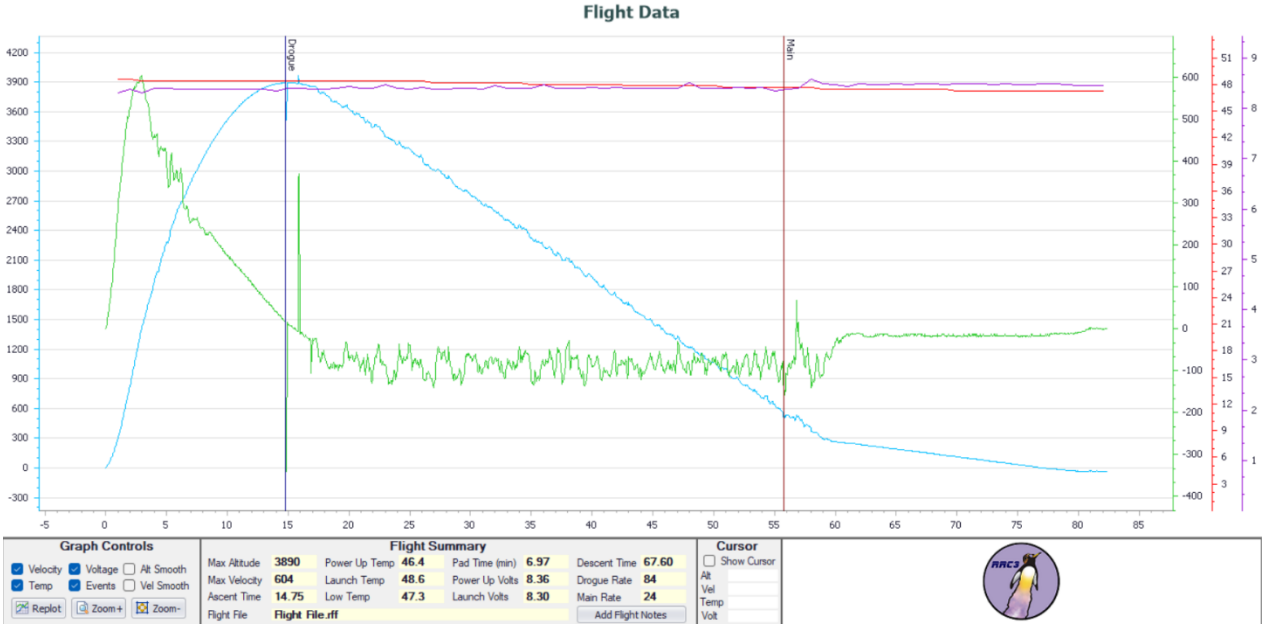

Figure 3.3.1. *Altimeter flight profile graph of Chariot flight #3 from primary RRC3 altimeter.*

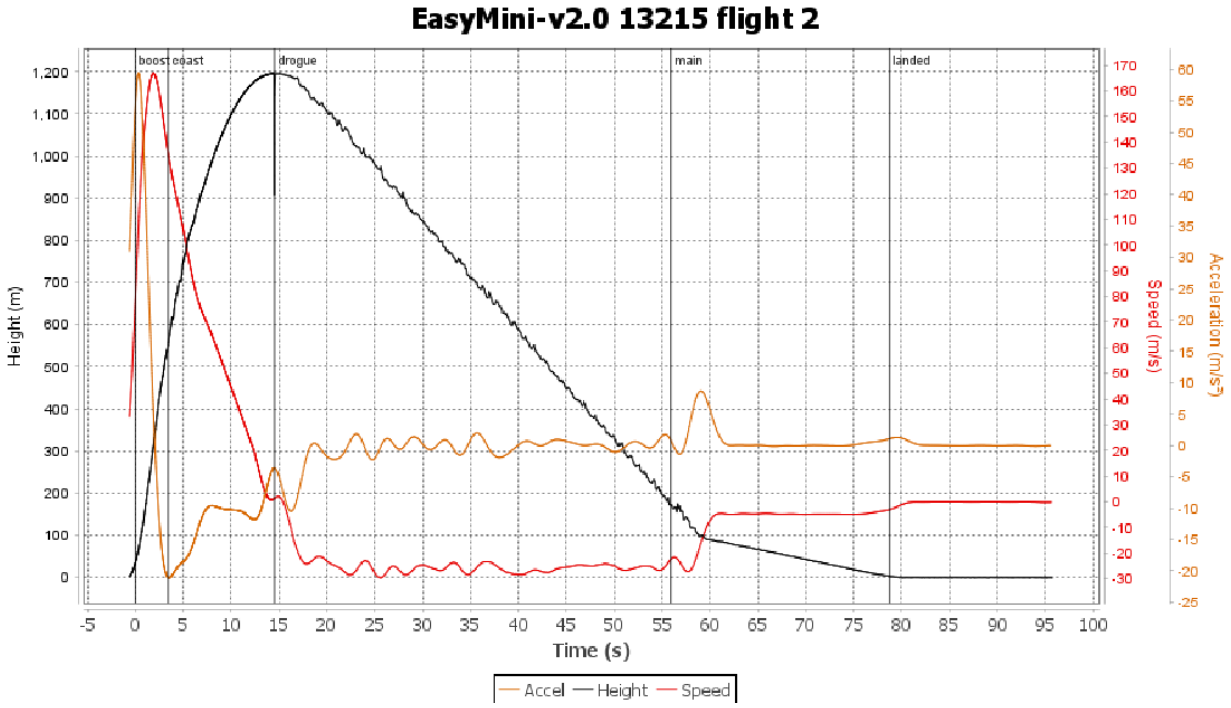

Figure 3.3.2. *Altimeter flight profile graph of Chariot flight #3 from secondary Easy mini altimeter.*

3.4. Vehicle Recovery Discussion

Chariot experienced a nominal recovery sequence during this third flight. The rocket landed 1,317 ft southeast of the launch site at a nominal velocity of 15.5 ft/s. Figure 3.4.1 contains an aerial view of the launch and landing sites and Figure 3.4.2 contains pictures of the gps receiver before and after launch verifying that the gps works as designed and transmits the location of chariot to the handheld receiver after the recovery sequence has been completed.

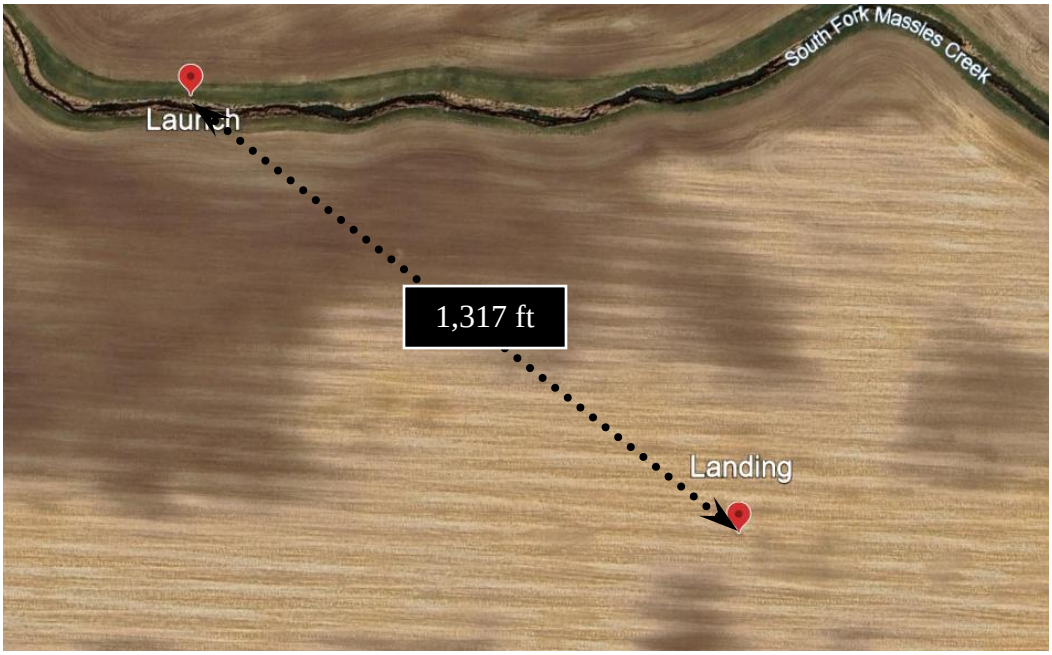

Figure 3.4.1. *Aerial view of launch and landing sites for Chariot flight #3. Chariot landed 1,317 ft from the launch rail.*

Figure 3.4.2. (Left) *Picture of Eggtimer gps reciever while Chariot is on the launch rail.* ***(Right)*** *Eggtimer gps receiver after landing.*

After landing, the aft section of Chariot was dragged along the ground for a few feet by the wind blowing the inflated main parachute as evidenced by an amount of mud being found inside the drogue parachute pay upon recovery. Nevertheless, Chariot sustained no damage during recovery. As landed photos of Chariot are recorded in Figures 3.4.3 through Figure 3.4.something below. Table 3.4.1 contains the actual kinetic energy of each section upon landing.

Figure 3.4.3. *As landed configuration of Chariot after flight #3 (drone view on right).*

Figure 3.4.4. *Chariot aft section as landed configuration.*

Figure 3.4.5. *Chariot avionics section as landed configuration.*

Figure 3.4.6. *Chariot forward section as landed configuration.*

Figure 3.4.7. *Chariot forward section and main parachute as landed configuration.*

Table 3.4.1. *Calculated kinetic energy of each independent section upon landing.*

Section	Forward	Avionics	Aft
Landng Velocity (ft/s)	15.5	15.5	15.5
Mass (slug)	0.207	0.124	0.386
Kinetic Energy (ft*lb)	24.85	14.85	46.43

3.5. Flight Analysis

Because the airbrakes were active and deployed during this launch the drag coefficient of the rocket was constantly changing during the coast phase of flight. Therefore, the drag coefficient of the rocket could not be calculated by plotting the velocity vs acceleration during the coast phase of flight and comparing it to the same curves generated in OpenRocket with varying drag coefficient. Instead, OpenRocket simulations of the pre- and post-flight rocket performance were compared as one method of verifying that Chariot is powerful enough to exceed the target altitude. Table 3.5.1 summarizes the flight performance under the real launch conditions from flight #3. Again, since the airbrakes system was active during the launch, these updated simulation results cannot be directly compared to Chariot's performance on 4/8/25.

Table 3.5.1. *Pre- and post-flight simulation summary.*

	Pre-Flight Simulated Value	Post-Flight Simulated Value
Temperature	60.0 F	44.6 F
Avg. Windspeed	0.0 ft/s	8.8 ft/s
Altitude	1063 ft	1063 ft
Pressure	0.947 bar	0.984 bar
Cd	0.574	0.574
Apogee	4478 ft	4400 ft
Velocity Off Rod	78.0 ft/s	77.9 ft/s
Max Velocity	557 ft/s	555 ft/s
Flight Time	75.4 s	73.5 s
Ground Hit Velocity	14.7 ft/s	13.8 ft/s

3.6. Future Flight Considerations

In terms of future hardware improvements, Chariot is not in need of any further major developments. However, CSL intends to expand its software development efforts to bring the airbrakes and primary payload to full operating potential. At least one, possibly two flights will be conducted before the final competition launch to 1) demonstrate full primary payload functionality and 2) demonstrate the airbrake control system's ability to augment the rocket's drag characteristics during the flight.